



## Synthesis of N-Doped Carbon Quantum Dots by Hydrothermal Synthesis Method and Investigation of Optical Properties

Sadiye Kübra BAŞKAYA<sup>1</sup>, Mustafa ÇEŞME<sup>2\*</sup>

<sup>1</sup> Department of Materials Science and Engineering, Graduate School of Natural and Applied Sciences, Kahramanmaraş Sütçü İmam University, Kahramanmaraş, Turkey

<sup>2</sup> Department of Chemistry, Faculty of Art and Sciences, Kahramanmaraş Sütçü İmam University, 46040, Kahramanmaraş, TURKEY

Sadiye Kübra BAŞKAYA ORCID No: 0000-0001-7940-3571

Mustafa ÇEŞME ORCID No: 0000-0002-2020-5965

\*Corresponding author: [mustafacesme@msn.com](mailto:mustafacesme@msn.com)

(Alınış: 23.06.2021, Kabul: 30.07.2021, Online Yayınlanma: 31.12.2021)

### Keywords

Carbon quantum dots, Spectroscopy, Cyclic voltammetry

**Abstract:** Carbon quantum dots (CQDs); It is a carbon-based nanomaterial that has become popular in recent years due to its advantages such as biocompatibility, tunable fluorescent properties, simple and economical synthesis methods. In this study, synthesis of N-doped carbon quantum dots by hydrothermal synthesis method using tangerine juice, onion shell and ethylenediamine was investigated. The structures and optical properties of the synthesized carbon quantum dots were illuminated by photoluminescence (PL), X-ray Diffractometer (XRD), Infrared (IR) and UV-vis spectrometer. Electrochemical properties were examined by the cyclic voltammetry (CV) technique. The stability of N-doped carbon quantum dots (at 1st, 10th, 15th and 26th days) and pH-dependent emission properties were investigated. Peaks are seen at 285 nm and 347 nm in the UV-vis spectrum proved the presence of C=O and C=N bonds. It has been observed that there is a redshift in the absorption peak due to the amine groups in the structure of the N-doped carbon quantum dots. As a result of the XRD analysis, it was seen that the N-doped carbon quantum dots were in an amorphous structure. The FTIR spectrum of N-doped carbon quantum dots characteristic absorption bands of shows N-H vibration stretching and C-H bending peaks at 3240 and 2923  $\text{cm}^{-1}$ , respectively. These functional groups seen in the structure showed that N-CQD is bonded by hydrogen bond. In 1574  $\text{cm}^{-1}$  and 1336  $\text{cm}^{-1}$  C=O vibration stretching peaks and C-N vibration stretching peaks are observed. In the next step, the electrochemical properties of the carbon dots were examined by cyclic voltammetry technique. Different scanning rates (10-1000 mV/s) were used to understand and clarify the substance (mass) transport to the electrode surface.

## Hidrotermal Sentez Yöntemi ile N-Katkılı Karbon Kuantum Noktaları Sentezi ve Optik Özelliklerinin Araştırılması

### Anahtar Kelimeler

Karbon kuantum noktaları, Spektroskopi, Dönüşümlü voltametri.

**Öz:** Karbon kuantum noktaları; biyoyumlu, ayarlanabilir floresan özellikler, basit ve ekonomik sentez yöntemleri gibi avantajlarından dolayı son yıllarda popüler hale gelen karbon tabanlı bir nanomalzemedir. Bu çalışmada mandalina suyu, soğan kabuğu ve etilendiamin kullanılarak hidrotermal sentez yöntemi ile N-katkılı karbon kuantum noktaları sentezi araştırılmıştır. Sentezlenen karbon kuantum noktalarının yapıları ve optik özellikleri fotoluminesans (PL), X-ray Difraktometresi (XRD), Kızılötesi (IR) ve UV-vis spektrometresi ile aydınlatılmıştır. Elektrokimyasal özellikleri ise dönüşümlü voltametri (CV) tekniği ile incelenmiştir. N-katkılı karbon kuantum noktalarının stabilitesi (1,10,15 ve 26. günlerde) ve pH bağımlı emisyon özellikleri araştırılmıştır. UV-vis spektrumunda 285 nm ve 347 nm' de görülen pikler C=O ve C=N bağlarının varlığını kanıtlamıştır. N-katkılı karbon kuantum noktalarının yapısındaki amin grupları nedeniyle absorpsiyon pikinde kırmızıya kayma olduğu gözlemlenmiştir. XRD analizi sonucunda N katkılı karbon kuantum noktalarının amorf yapıda olduğu görüldü. N-katkılı karbon kuantum noktalarının FTIR spektrumu, sırasıyla 3240 ve 2923  $\text{cm}^{-1}$  de N-H titreşim gerilmesini ve C-H bükülme piklerini gösterir. Yapıda görülen bu fonksiyonel gruplar, N-CQD'nin hidrojen bağı ile bağlandığını göstermiştir. 1574  $\text{cm}^{-1}$  ve 1336  $\text{cm}^{-1}$  de C=O titreşim uzama pikleri ve C-N titreşim uzama pikleri gözlenmektedir. Bir sonraki adımda N-CQD'lerin elektrokimyasal davranışı dönüşümlü voltametri tekniği ile incelenmiştir. Elektrot yüzeyinde madde (kütle) taşınımını anlamak ve netleştirmek için farklı tarama hızları (10-1000 mV/s) kullanılmıştır.

## 1. INTRODUCTION

Nanomaterials are colloidal particles with significant physicochemical and optoelectronic properties ranging in size from 1 to 100 nm. The multi-functionality of these particles has made them usable in many areas [1]. Carbon is one of the elements abundant in the universe, which has a large number of allotropes. Carbon family nanomaterials are carbon nanofibers, nanotubes, nano diamond, graphene, fullerene, and carbon quantum dots (CQDs) [2–5].

CQDs are a new division of carbon-based nanomaterials with dimensions below 10 nm, discovered in 2004. It has high photostability, tunable fluorescent properties, biocompatibility and good water dissolution properties. It also has low toxicity and chemical inertness. For this reason, they are used in drug delivery systems, bioimaging and photodynamic therapy. Due to their easy functionalization and excellent photoluminescence properties are also used in sensor applications in different fields such as nanomedicine and optoelectronics [6–8].

CQDs are thought to be potential candidates to replace conventional semiconductor quantum dots in the future due to their advantages [3,9]. The morphologies of carbon quantum dots are mostly hemispherical. Their structures can be amorphous, graphitic or  $C_3N_4$  crystalline core [10,11]. Functional groups found in carbon quantum dots have given them various properties. Some of these are good solubility in water and easily functionalized with different species. In addition, functional groups on the surface of carbon quantum dots increase their optical properties, biocompatibility, and targeting properties [12–14].

Carbon quantum dots are synthesized by two different methods: top-down and bottom-up. Top-down methods involve the breakdown of large carbon materials. These methods involve laser ablation, arc discharge, electrochemical techniques, and high-energy ball milling methods. The bottom-up synthesis methods are used to synthesize CQD from small molecules via carbonization and passivation. These synthesis methods are hydrothermal, solvothermal, microwave-assisted methods, ultrasonic-assisted methods, combustion, and chemical vapor deposition [14,15]. In bottom-up synthesis methods, precursors such as saccharides, amino acids and biopolymers are widely used [16,17].

Nitrogen-doped carbon quantum dots are of great interest among carbon quantum dots due to their advantages, such as highly developed photoluminescence properties, specific properties, and applications. Furthermore, N-doped carbon quantum dots and carbon quantum dots are also used in bioimaging in sensor applications such as the determination of metal ions due to their easy synthesis, economical, eco-friendly, tunable fluorescence properties and high quantum efficiency [18–20]. In this study, nitrogen-doped CQDs synthesis has been successfully carried out using tangerine juice, onion shell

and ethylenediamine. Furthermore, the structures of the synthesized N-doped carbon quantum dots were elucidated using various spectroscopy and electrochemical techniques. The N-doped CQDs synthesized will shed light on future carbon quantum dots synthesis studies.

## 2. MATERIALS AND METHODS

### 2.1. Apparatus and Reagents

Tangerine juice and onion shell were used as carbon sources. Samples were purchased from the local market. It was obtained Sigma Aldrich from ethylenediamine used as nitrogen additive. UV-vis absorption spectra were measured with Shimadzu-1800 UV-vis spectrometer, photoluminescence (PL) spectrum was measured with Varian Cary Eclipse spectrometer. Infrared spectroscopy (FTIR) was performed with Perkin Elmer Spectrum 400. XRD analysis was performed with Philips X'Pert PRO XRD. The Hitachi HT7700 with EXALENS, 120 kV, the electron microscope was used to record the transmission electron microscopy (TEM). pH measurements were made with Thermo Scientific A215.

### 2.2. The Synthesis of N-Doped Carbon Quantum Dots

Onion shells were dried in an oven at 50°C. The drying substance was ground and pulverized. The tangerines were squeezed out of the juice. A solution was prepared using 50 mL of tangerine juice, 1 g of onion shell and 1 mL of ethylenediamine (EDA). The solution was mixed in a magnetic stirrer for 15 minutes. The hydrothermal synthesis method was used for the synthesis of carbon quantum dots. 50 mL Teflon-lined steel autoclave was used for the hydrothermal synthesis method. The prepared solution was transferred to the autoclave and left to the synthesis process at 180°C and 2 hours reaction time. After the reaction, the obtained product was filtered and centrifuged for 10 min at 15000 rpm. After centrifugation, it was dried at 50 °C in the oven.

### 2.3. Electrochemical Procedure

In this study was used the cyclic voltammetry technique (CV). A glassy carbon electrode was used as working electrode, Ag/AgCl electrode as a counter electrode and platinum wire as the auxiliary electrode. The working electrode was pretreated by polishing it with aluminum oxide ( $Al_2O_3$ ) powder. After pretreatment, the electrode was washed with deionized water and then dried and placed in the cell. After each experiment, the auxiliary electrode and reference electrode were cleaned with distilled water, dried, and placed back into the cell. 0.3 M Tris buffer was used as the electrolyte in the pH at 7.4.

### 3. RESULTS AND DISCUSSION

The absorption behavior of carbon quantum dots was investigated by UV-vis spectroscopy. The UV-vis spectrum for carbon quantum dots is given in (Figure 1). In addition, the image of the synthesized N-doped carbon quantum dots under UV light with a wavelength of 365 nm and the daylight image are given in (Figure 1). CDs UV-vis spectra gave distinct peaks at 285 nm and 347 nm. These peaks show the C=O and C=N bonds, respectively, and can be said to make  $n-\pi^*$  transitions. It can be concluded that there is a red shift in the absorption peak due to the amine groups present in the N-doped carbon quantum points [20–22].

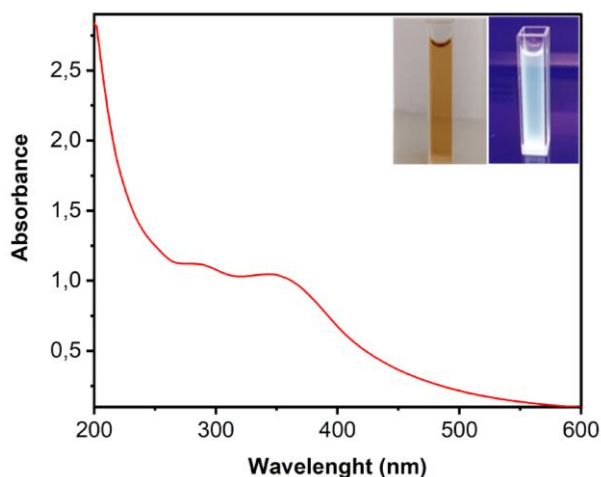


**Figure 1.** UV-Vis spectrum of N-CQD, inset image shows the solution of prepared N-CQD under daylight and UV light.

The crystal structures of carbon quantum dots were examined by XRD analysis (Figure 2). A distinct diffraction peak was observed at  $23.35^\circ$  in the XRD spectrum. This diffraction peak indicates that carbon quantum dots are of amorphous structure.

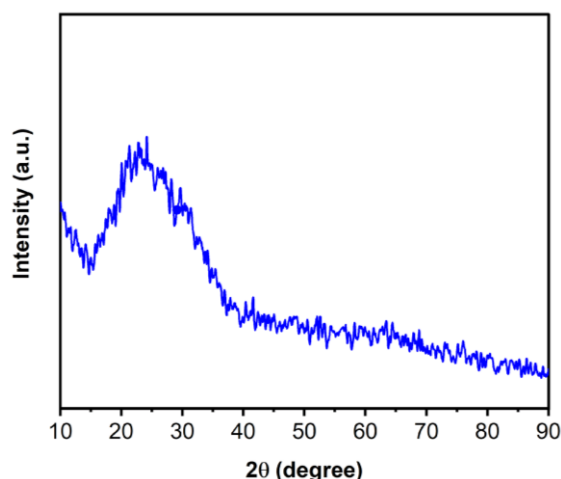


**Figure 2.** XRD diffraction pattern of the N-CQD.

The photoluminescence emission spectrum of the N-doped carbon quantum dots excitation, emission and density values is given in (Figure 3). It has been observed that when the excitation wavelength is risen from 300 nm to 400 nm, the emission intensity of N-doped carbon quantum dots increases and when excited

at 338 nm, it gives the maximum emission value. At this point, the highest fluorescence intensity was found to be 416. This result means that the varying excitation wavelength leads to adjustable emission spectra and can be caused by carbon nuclei and supporting functional groups and uniform and non-uniform dimensional CDs.

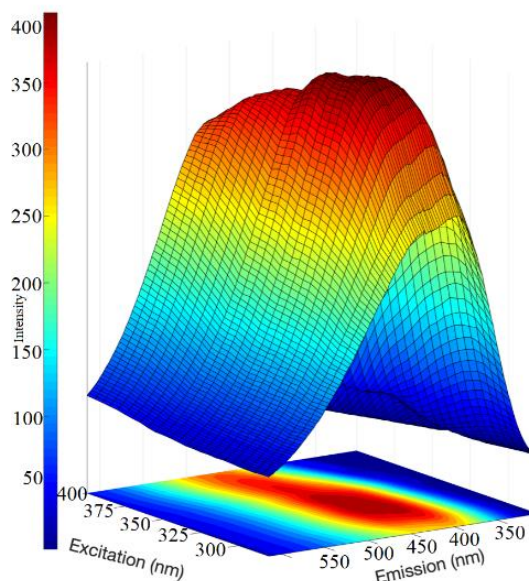


**Figure 3.** Excitation depended on PL spectra of synthesized N-CQD.

Functional groups in the structure of carbon quantum dots are shown by infrared spectroscopy (IR). In the FT-IR spectrum given in (Figure 4), the absorption band of  $3240\text{ cm}^{-1}$  and  $2923\text{ cm}^{-1}$  shows the N-H and C-H vibration stretching peaks, respectively. From here, it can be concluded that a hydrogen bond binds N-CQD. C=O, C-N and C-O vibration stretching peaks were observed in the absorption band of  $1574\text{ cm}^{-1}$  and  $1336\text{ cm}^{-1}$  and  $1038\text{ cm}^{-1}$ , respectively [18,22,23].

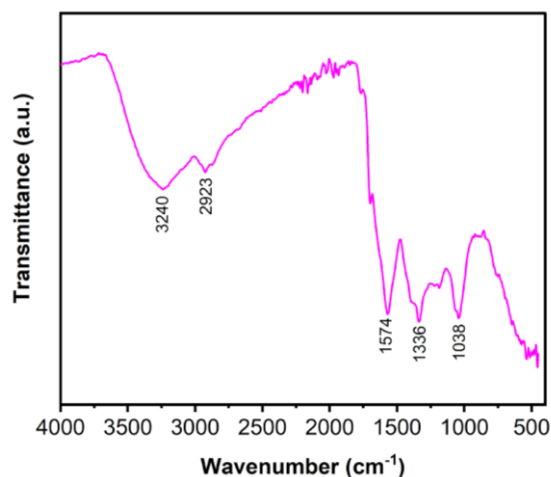


**Figure 4.** FT-IR spectrum of N-CQD.

The TEM image confirmed the synthesis of CQDs and their morphological properties were investigated. According to the TEM image given in (Figure 5), N-doped carbon quantum dots are spherical and monodisperse. Furthermore, it was observed that the synthesized N-doped carbon quantum dots had a narrow dimensional diameter distribution, had an average

diameter of 21.33 nm, and had similar morphological structures.

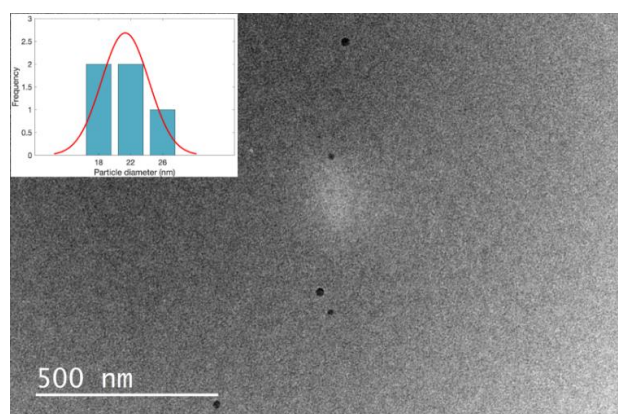


**Figure 5.** TEM spectrum of N-doped carbon quantum dots. inset graph shows the average diameter of CQDs.

The change of carbon quantum dots at different pH ranges is given in (Figure 6). Acidic pH values were adjusted with 0.1M HCl solution, and basic pH values were adjusted with 0.1M NaOH solution. It was observed that the peak intensity was maximum at pH=4.87. On the other hand, it was observed that the peak intensity was the least at pH=7.2 and increased at pH=11.26.

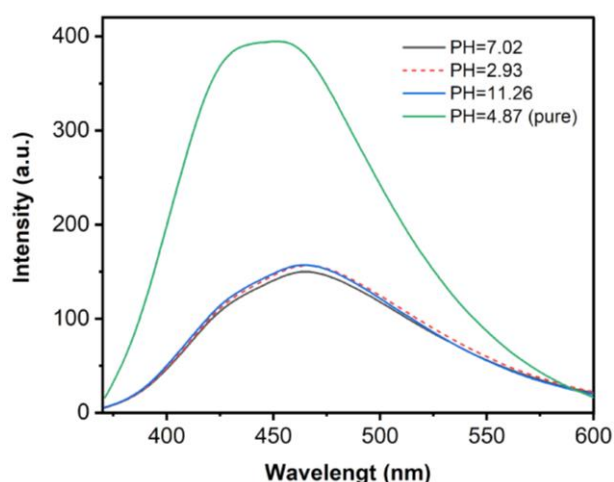


**Figure 6.** pH spectrum of N-doped carbon quantum dots.

The photoluminescence spectrum of carbon quantum dots measured on different days is given in (Figure 7). For stability study, the sample was kept in the cold medium. Here, it is seen that the peak intensity decreased on the 10th day compared to the 1st day, and the peak intensity continued to decrease on the 10th day and afterward but became stable after a specific time. The results obtained for stability show that carbon quantum dots can be applied in biological applications.

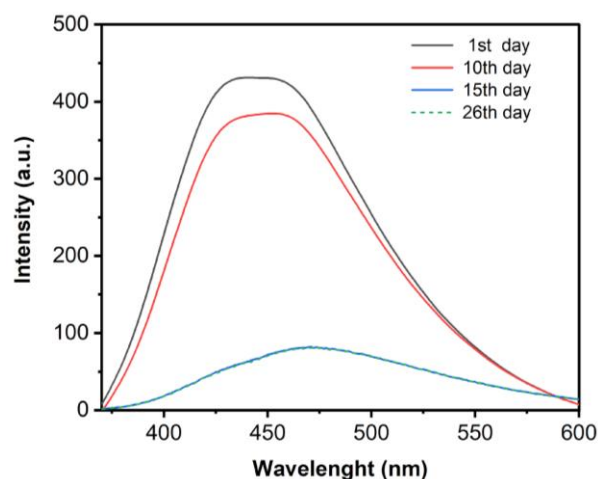


**Figure 7.** Stability spectrum of N-doped carbon quantum dots.

The electrochemical properties of N-doped CDs were analyzed by cyclic voltammetry technique after characterization was performed through UV-vis, FT-IR, and photoluminescence spectroscopy. The CV technique has been worked cyclic between -2000 and +2000 mV for the potential sweep. Different scanning rates (10-1000 mV/s) were used to understand and clarify the substance (mass) transport to the electrode surface. In scanning rate studies, measurements of up to 1000 mV/s have been taken, but anodic peak current has begun to decrease, especially at measurements with a decreasing scanning rate lower than 50 mV/s. Figure 8 shows the usual cyclic voltammograms (CV) curves in 0.1 M PBS solution. As shown in the figure, the peak currents gradually increased with increasing scan rates and similarly decreased as the scan rate decreased. For measurements taken at 100 mV/s, the anodic peak current; is around 447 mV. No significant peak current was observed in the cathodic direction. The peak observed around 447 mV at 100 mV/s scanning rate in the anodic direction decreased to 190 mV at 50 mV/s rate.

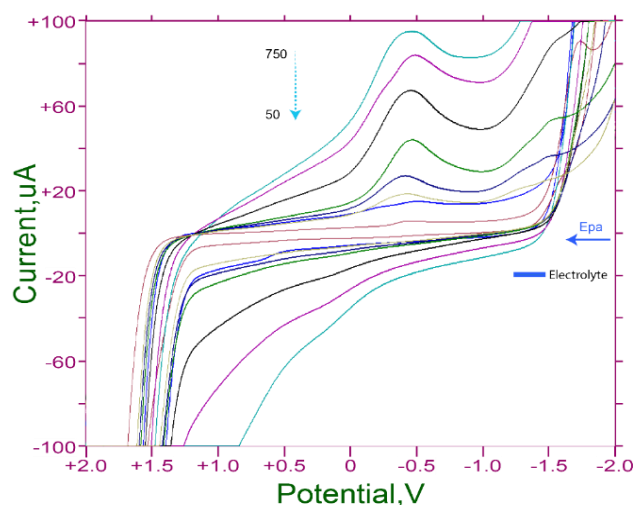


**Figure 8.** The scan rate (50–750 mV/s) effect on peak current of CQDs in 0.3 M Tris buffer at pH 7.4

Graphs describing the relationship between peak currents and scan rates shown in Figures 9 A and B were obtained from the voltammograms of Figure 8. The

linearity of the peak current ( $I_p$ ) depending on the square root of the scan rate was obtained by the electrode, demonstrating a diffusional behavior. These relations are stated as equations below.

$$i_{pa} (\mu A) = 3.675 v^{1/2} (mVs^{-1}) + 0.5964, R^2: 0.9892$$

In similar scan rates, the effect of scan rates on peak current were also analyzed with a graph of the logarithm of peak current vs. scan rates logarithm that gives a straight line. These linear relations were acquired as follows (Figure 9);

$$\log_{ia} (\mu A) = 0.5216 \log v (mVs^{-1}) + 0.5176, R^2: 0.9843$$

According to these results, the relationship between the logarithm of the potential scanning rates and the logarithm of the peak current is about 0.52, and these values are close to 0.5, which is the theoretical value, that indicates the substance transport on the electrode surface by diffusion [24].

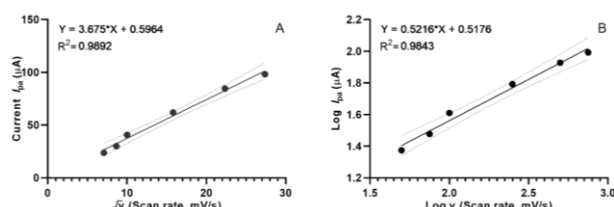


**Figure 9.** The linear relation between peak current and the square root of the scan rate; (A) anodic, (B), Plot of peak current vs. log of scan rate.

#### 4. CONCLUSION

In this study, N-doped carbon quantum dots were synthesized using tangerine juice, onion shell, and ethylenediamine. The hydrothermal method, which is quite economical and straightforward, was used for the synthesis process. Reaction: It was carried out at a temperature of 180°C and a reaction time of 2 hours. The structure and optical properties of the synthesized N-doped carbon quantum dots were illuminated by UV-vis, photoluminescence (PL), infrared spectroscopies (IR) and crystal structure by XRD analysis. Electrochemical properties of carbon quantum dots investigated the cyclic voltammetry technique. In addition, the stability of carbon quantum dots and the pH effect in acidic, basic, and neutral environments were investigated.

#### Acknowledgments

This work was financially supported by the Kahramanmaraş Sütçü İmam University Scientific Research Project Coordination Unit (Project Number: 2019/5-21 M and 2020/7-9 D).

#### REFERENCES

- [1] N. Tejwan, S.K. Saha, J. Das, Multifaceted applications of green carbon dots synthesized from renewable sources, *Adv. Colloid Interface Sci.* 275 (2020) 102046. <https://doi.org/10.1016/j.cis.2019.102046>.
- [2] X. Wang, Y. Feng, P. Dong, J. Huang, A Mini Review on Carbon Quantum Dots: Preparation, Properties, and Electrocatalytic Application, *Front. Chem.* 7 (2019). <https://doi.org/10.3389/fchem.2019.00671>.
- [3] H. Eskalen, Influence of carbon quantum dots on electro-optical performance of nematic liquid crystal, *Appl. Phys. A.* 126 (2020) 708. <https://doi.org/10.1007/s00339-020-03906-7>.
- [4] H. Eskalen, S. Uruş, S. Cömertpay, A.H. Kurt, Ş. Özgan, Microwave-assisted ultra-fast synthesis of carbon quantum dots from linter: Fluorescence cancer imaging and human cell growth inhibition properties, *Ind. Crops Prod.* 147 (2020) 112209. <https://doi.org/10.1016/j.indcrop.2020.112209>.
- [5] H. Eskalen, M. Çeşme, S. Kerli, Ş. Özgan, Green synthesis of water-soluble fluorescent carbon dots from rosemary leaves: Applications in food storage capacity, fingerprint detection, and antibacterial activity, *J. Chem. Res.* 45 (2021) 428–435. <https://doi.org/10.1177/1747519820953823>.
- [6] C.M. Galanakis, Recovery of high added-value components from food wastes: Conventional, emerging technologies and commercialized applications, *Trends Food Sci. Technol.* 26 (2012) 68–87. <https://doi.org/10.1016/j.tifs.2012.03.003>.
- [7] K.K. Chan, S.H.K. Yap, K.T. Yong, Biogreen Synthesis of Carbon Dots for Biotechnology and Nanomedicine Applications, *Nano-Micro Lett.* 10 (2018) 72. <https://doi.org/10.1007/s40820-018-0223-3>.
- [8] S. Jayaweera, K. Yin, X. Hu, W.J. Ng, Fluorescent N/Al Co-Doped Carbon Dots from Cellulose Biomass for Sensitive Detection of Manganese (VII), *J. Fluoresc.* 29 (2019) 1291–1300. <https://doi.org/10.1007/s10895-019-02452-7>.
- [9] A. Prasanna, T. Imae, One-pot synthesis of fluorescent carbon dots from orange waste peels, *Ind. Eng. Chem. Res.* 52 (2013) 15673–15678. <https://doi.org/10.1021/ie402421s>.
- [10] A. Sciortino, A. Cannizzo, F. Messina, Carbon Nanodots: A Review—From the Current Understanding of the Fundamental Photophysics to the Full Control of the Optical Response, *J. Carbon Res.* 4 (2018) 67. <https://doi.org/10.3390/c4040067>.
- [11] J. Woo, Y. Song, J. Ahn, H. Kim, Green one-pot preparation of carbon dots (CD)-embedded cellulose transparent film for Fe<sup>3+</sup> indicator using ionic liquid, *Cellulose.* 27 (2020) 4609–4621. <https://doi.org/10.1007/s10570-020-03099-5>.
- [12] L. Liu, Y. Li, L. Zhan, Y. Liu, C. Huang, One-step synthesis of fluorescent hydroxyls-coated carbon dots with hydrothermal reaction and its application to optical sensing of metal ions, *Sci. China Chem.* 54 (2011) 1342–1347. <https://doi.org/10.1007/s11426-011-4351-6>.
- [13] S. Ahmadian-Fard-Fini, M. Salavati-Niasari, D. Ghanbari, Hydrothermal green synthesis of magnetic Fe<sub>3</sub>O<sub>4</sub>-carbon dots by lemon and grape fruit extracts and as a photoluminescence sensor for detecting of E. coli bacteria, *Spectrochim. Acta - Part A Mol. Biomol. Spectrosc.* 203 (2018) 481–493. <https://doi.org/10.1016/j.saa.2018.06.021>.

- [14] M.J. Molaei, Principles, mechanisms, and application of carbon quantum dots in sensors: A review, *Anal. Methods*. 12 (2020) 1266–1287. <https://doi.org/10.1039/c9ay02696g>.
- [15] A. Nair, J.T. Haponiuk, S. Thomas, S. Gopi, Natural carbon-based quantum dots and their applications in drug delivery: A review, *Biomed. Pharmacother.* 132 (2020) 110834. <https://doi.org/10.1016/j.biopha.2020.110834>.
- [16] N. Papaioannou, M.M. Titirici, A. Sapelkin, Investigating the Effect of Reaction Time on Carbon Dot Formation, Structure, and Optical Properties, *ACS Omega*. 4 (2019) 21658–21665. <https://doi.org/10.1021/acsomega.9b01798>.
- [17] Z. Song, F. Quan, Y. Xu, M. Liu, L. Cui, J. Liu, Multifunctional N,S co-doped carbon quantum dots with pH- and thermo-dependent switchable fluorescent properties and highly selective detection of glutathione, *Carbon N. Y.* 104 (2016) 169–178. <https://doi.org/10.1016/j.carbon.2016.04.003>.
- [18] R. Atchudan, T.N.J.I. Edison, D. Chakradhar, S. Perumal, J.J. Shim, Y.R. Lee, Facile green synthesis of nitrogen-doped carbon dots using *Chionanthus retusus* fruit extract and investigation of their suitability for metal ion sensing and biological applications, *Sensors Actuators, B Chem.* 246 (2017) 497–509. <https://doi.org/10.1016/j.snb.2017.02.119>.
- [19] G. Muthusankar, R.K. Devi, G. Gopu, Nitrogen-doped carbon quantum dots embedded Co<sub>3</sub>O<sub>4</sub> with multiwall carbon nanotubes: An efficient probe for the simultaneous determination of anticancer and antibiotic drugs, *Biosens. Bioelectron.* 150 (2020) 111947. <https://doi.org/10.1016/j.bios.2019.111947>.
- [20] P. Wu, W. Li, Q. Wu, Y. Liu, S. Liu, Hydrothermal synthesis of nitrogen-doped carbon quantum dots from microcrystalline cellulose for the detection of Fe<sup>3+</sup> ions in an acidic environment, *RSC Adv.* 7 (2017) 44144–44153. <https://doi.org/10.1039/c7ra08400e>.
- [21] Z.F. Pu, Q.L. Wen, Y.J. Yang, X.M. Cui, J. Ling, P. Liu, Q.E. Cao, Fluorescent carbon quantum dots synthesized using phenylalanine and citric acid for selective detection of Fe<sup>3+</sup> ions, *Elsevier B.V.*, 2020. <https://doi.org/10.1016/j.saa.2019.117944>.
- [22] P.F. Andrade, G. Nakazato, N. Durán, Additive interaction of carbon dots extracted from soluble coffee and biogenic silver nanoparticles against bacteria, *J. Phys. Conf. Ser.* 838 (2017). <https://doi.org/10.1088/1742-6596/838/1/012028>.
- [23] Y. Hu, X. Geng, L. Zhang, Z. Huang, J. Ge, Z. Li, Nitrogen-doped Carbon Dots Mediated Fluorescent on-off Assay for Rapid and Highly Sensitive Pyrophosphate and Alkaline Phosphatase Detection, *Sci. Rep.* 7 (2017) 1–9. <https://doi.org/10.1038/s41598-017-06356-z>.
- [24] J. Wang, *Analytical Electrochemistry*, Third Edition, John Wiley & Sons, Inc., Hoboken, NJ, USA, 2006. <https://doi.org/10.1002/0471790303>.